Journal of Magnetic Resonance **145,** 142–146 (2000)
doi:10.1006/jmre.2000.2091, available online at http://www.idealibrary.com on IDEAL®

COMMUNICATIONS

Hydrogen Bonding Effects on the ^{15}N and ^{1}H Shielding Tensors in Nucleic Acid Base Pairs

Jiří Czernek,[1] Radovan Fiala, and Vladimír Sklenář[2]

Laboratory of Biomolecular Structure and Dynamics, Masaryk University, Kotlářská 2, CZ-611 37 Brno, Czech Republic

Received December 13, 1999; revised March 20, 2000

The results of systematic *ab initio* calculations of ^{15}N and ^{1}H chemical shielding tensors in the GC base pair as a function of hydrogen bond length are presented for the first time. The hydrogen bond length characterized by the distance $r_{N\cdots N}$ between purine N1 and pyrimidine N3 was varied between 2.57 and 3.50 Å and the chemical shift tensors were calculated by the sum-over-states density functional perturbation theory. It is shown that the hydrogen bond length has a strong effect on the chemical shielding tensor of both imino proton and nitrogen, on their orientation, and, as a consequence, on the relaxation properties of both nuclei. For a nitrogen nucleus not involved in hydrogen bonding, the shielding tensor is nearly axially symmetric and almost collinear with the bond vector. As the length of the hydrogen bond decreases, the least shielding component σ_{11} deflects from the N–H vector and the shielding tensor becomes increasingly asymmetric. The significance of the presented results for the analysis of relaxation data and the efficiency of TROSY effects together with a summary of the relevant shielding parameters are presented and discussed.

Key Words: **NMR; chemical shielding tensor; *ab initio* calculations; purines; pyrimidines; TROSY; relaxation.**

During past few years, the ^{15}N isotope has become a prominent messenger of biopolymer dynamics (*1*) in proteins and nucleic acids. Successful interpretation of ^{15}N NMR relaxation data requires an accurate knowledge of the chemical shift anisotropy (CSA). So far, the ^{15}N relaxation data has been interpreted based on assumptions that the ^{15}N shielding tensor is axially symmetric, its axis of symmetry is collinear with the ^{15}N–^{1}H dipolar tensor, and the CSA values are uniform throughout the molecule. These assumptions, however, are not generally valid. As shown recently for noncollinear tensors, highly anisotropic molecular rotation results in differences in site-specific correlation functions and spectral densities (*2, 3*). In addition, the noncollinearity significantly affects the efficiency of dipolar and CSA compensation in TROSY experiments (*4, 5*).

The hydrogen bonding effects on the ^{1}H isotropic chemical shift have been known, and understood in a qualitative fashion, for a long time (*6*). A detailed examination (*7*) of 77 A, B, and Z DNA crystal structures revealed that imino hydrogen bond length (N···N) varied between 2.7 and 3.1 Å with a small number of very short values (2.2–2.6 Å). The observation of variations in ^{15}N–^{15}N scalar couplings ($^{2}J_{NN}$) across the Watson–Crick base pairs (*8, 9*), and *ab initio* calculations of the $^{2}J_{NN}$ dependence on the N···N distance indicates that the length of a hydrogen bond also changes in solution. The recently published methods (*2*) determining ^{15}N CSA and θ indirectly from the measured relaxation data open up a possibility to assess the length of the NH···H hydrogen bond providing the distance dependence of the ^{15}N chemical shielding parameters can be established independently. Since the influence of hydrogen bond length on ^{1}H and ^{15}N shielding anisotropy cannot be studied experimentally in a systematic way, the theoretical approach remains the only possibility. For proteins, *ab initio* methodology on the DFT level was applied to follow the changes in CSA, in a model consisting of two *N*-methylacetamide molecules, as a function of the C═O···H–N distance (*10*). Here the N anisotropy only changed by about 5 ppm (except for the distances below 2.0 Å), whereas both the H and C anisotropies were very sensitive to nearby groups. Recently, the principal values of ^{15}N chemical shielding tensors in uracil (*11*) and adenine, cytosine, guanine, and thymine (*12*) have been measured using solid state NMR and their assignments assisted by *ab initio* methods. The results indicate that calculations comprising intermolecular interactions produce σ_{ii} values in substantially better agreement with the experimental data.

Here we present the first results of systematic *ab initio* calculations of ^{15}N and ^{1}H chemical shielding tensors in nucleic acid base pairs as a function of hydrogen bond length. As will be demonstrated for a GC base pair, the hydrogen bond length has a strong influence on the chemical shielding tensor

[1] Present address: Institute of Macromolecular Chemistry, Academy of Science of the Czech Republic, Heyrovského nám. 2, 162 06 Praha 6, Czech Republic.

[2] To whom correspondence should be addressed E-mail: sklenar@chemi.muni.cz.

1090-7807/00 $35.00

of both imino proton and nitrogen, on their orientation and, as a consequence, on the relaxation properties of both nuclei.

We used the geometry of a CG pair from the crystal structure (*13*) deposited in the NDB resource (ID: BDL001). The geometry, except for the hydrogen bond length, was not further modified to isolate the direct effects on the computed parameters from those arising indirectly due to the changes in geometry in the process of the computational optimization. To speed up the computation, the sugar residue was replaced by a hydrogen atom. The hydrogen bond length characterized by the distance $r_{N\ldots N}$ between purine N1 and pyrimidine N3 was varied between 2.57 and 3.50 Å by a translation along the direction of the GN1–CN3 axis. The chemical shift tensors were calculated using sum-over-states density functional perturbation theory with the IGLO gauge choice (SOS-DFPT-IGLO) as implemented in deMon-MASTER-CS code (*14, 15*). The Perdew–Wang-91 exchange-correlation potential (*16, 17*), the approximation Loc. 1 SOS-DFPT (*18, 19*), and the basis set of IGLO-III of Kutzelnigg *et al.* (*20*) were used. To verify the accuracy of the SOS-DFPT-IGLO data obtained, selected calculations were also performed using the GAUSSIAN94 suite of programs (*21*). The DFT-GIAO (*22*) method (hybrid B3LYP functional (*23*) with TZ2P basis set (*24*)) was employed. This approach has been shown (*25*) to produce virtually same ^{1}H and ^{13}C chemical shifts as PW91/IGLO-III in the framework of SOS-DFPT-IGLO, but at a considerably higher computational cost. An analogous situation also was observed for ^{15}N and ^{1}H shielding tensors studied here. The differences between the two methods were less than 2.1 ppm and 2.8° for δ_N and θ_N, respectively. The time requirements on the SGI Power Challenge computer with R10000 processor for the given calculation were approximately 15 h for SOS-DFPT-IGLO and 70 h for DFT-GIAO, clearly favoring the SOS-DFPT-IGLO methodological approach.

The basis set dependence, the influence of the relaxation of the base pair geometry with changing $r_{N\ldots N}$, and the basis set superposition error are the most important factors that in principle could affect the accuracy of the chemical shielding tensors. All three factors have been studied in detail. As will be presented elsewhere, none of these problems affect the validity of the results discussed below.

There has been a lot of inconsistency in the literature in the usage of terms and symbols regarding the phenomenon of chemical shielding. In this paper, we use the term and symbol definitions as described in the following paragraphs.

Chemical shielding and chemical shift are tensors of rank 2. $\sigma_{11} \leq \sigma_{22} \leq \sigma_{33}$ are the components of the diagonalized shielding tensor. The same symbols are often used for the components of the chemical shift tensor that we denote here by δ_{nn}. The element δ_{11} represents the largest shift component, as $\delta_{nn} = \sigma_{ref} - \sigma_{nn}$. Since the anisotropy parameters are calculated as differences of the tensor components, they are independent of the reference and therefore can be calculated either from the shifts or from the shieldings. For consistency, indexes 11 and 33 should be switched when the shifts are substituted for shieldings and vice versa. $\sigma_{iso} = (\sigma_{11} + \sigma_{22} + \sigma_{33})/3$ is the isotropic chemical shielding, and $\delta = \sigma_{ref} - \sigma_{iso}$ is the isotropic chemical shift, where σ_{ref} is the isotropic shielding of a reference nucleus. Chemical shift anisotropy is a scalar quantity defined for an axially symmetric shielding tensor as the difference between the shielding of the nucleus under study when the static magnetic field is parallel, $\sigma_\parallel$, and when the field is orthogonal, $\sigma_\perp$, to the axis of symmetry of the shielding tensor.

$$\mathrm{CSA} = \sigma_\parallel - \sigma_\perp \qquad [1]$$

CSA characterizes the (auto)relaxation processes. If the axis of symmetry of the shielding tensor is not parallel with the internuclear vector, the cross-correlation rate between CSA and DD depends on the parameter $\Delta\sigma^*$

$$\Delta\sigma^*_{sym} = \mathrm{CSA}(3\cos^2\theta - 1)/2, \qquad [2]$$

where θ is the angle between the internuclear vector and the axis of the shielding tensor, and the subscript sym indicates an axially symmetric shielding tensor.

In the case of a nonsymmetric shielding tensor, the above approach is not directly applicable, as there is no preferable direction of the shielding. By analogy, we can define a parameter $\Delta\sigma$ as

$$\Delta\sigma = \sigma_{11} - (\sigma_{22} + \sigma_{33})/2 \qquad [3]$$

and the asymmetry factor

$$\Delta\eta = (\sigma_{22} - \sigma_{33})/(\sigma_{11} + \sigma_{iso}). \qquad [4]$$

In the axially symmetric case, $\Delta\sigma = \mathrm{CSA}$ and $\Delta\eta = 0$ as long as we chose σ_{33} to be parallel to the axis of symmetry of the tensor rather than as the most shielded component.

If the shielding tensor lacks the axial symmetry, the effective anisotropy contributing to the relaxation is characterized by

$$\mathrm{CSA}_a = \Delta\sigma(1 + \Delta\eta^2/3)^{1/2}. \qquad [5]$$

Since CSA_a has the same physical meaning as CSA defined for the axially symmetric case, we denote it as the chemical shift anisotropy with an index a indicating that the tensor is asymmetric. Alternatively, we can characterize the relaxation properties using the effective $\Delta\sigma$ (*26*) defined as

$$\Delta\sigma_{eff} = (\sigma_{11}^2 + \sigma_{22}^2 + \sigma_{33}^2 - \sigma_{11}\sigma_{22} - \sigma_{11}\sigma_{33} - \sigma_{22}\sigma_{33})^{1/2}. \qquad [6]$$

The last two expressions are equivalent in the sense that $|\mathrm{CSA}_a| = \Delta\sigma_{eff}$. While $\Delta\sigma_{eff}$ is always positive, CSA_a can be either

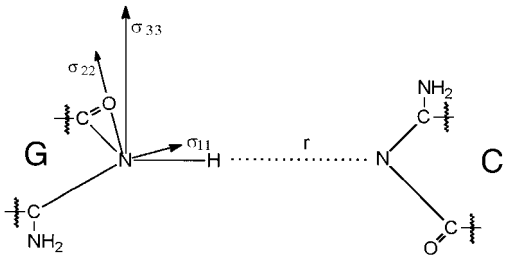

FIG. 1. Orientation of the chemical shielding tensor of the guanine imino nitrogen in a G–C base pair.

positive or negative. This difference is rather academic, though, since the terms always appear as squares in the relaxation equations.

Unlike the (auto)relaxation, the cross-correlation rate depends also on the orientation of the shielding tensor with respect to the internuclear axis. In a general case

$$\Delta\sigma^*_{\text{eff}} = \sigma_{11}(3\cos^2\theta_{11} - 1)/2 + \sigma_{22}(3\cos^2\theta_{22} - 1)/2 + \sigma_{33}(3\cos^2\theta_{33} - 1)/2, \quad [7]$$

where θ_{nn} is the angle between the corresponding component of the tensor and the internuclear vector.

Figure 1 shows the orientation of the chemical shielding tensor principal axes in a GC base pair for a typical hydrogen bond length (*27*) $r_{N\ldots N}$ = 2.87 Å. The SOS-DFPT-IGLO results are summarized in Table 1.

The calculated isotropic chemical shifts of both the imino nitrogen and the proton decrease with the increasing distance between G and C. This is in agreement with experimental values. For example, in the ATP-binding aptamer (*28*), the chemical shifts of the imino proton and nitrogen for the base-paired G6 in the stem are δ_H = 11.74 and δ_N = 147.0 ppm, while for the bulged-out G34, which has a limited opportunity to create hydrogen bonds, the corresponding values are 10.33 and 143.2 ppm, respectively. The tendency is easily understood in terms of the weakening of the hydrogen bond with distance. The longer the hydrogen bond, the higher the shielding of the imino group (as a result of decreasing charge transfer between G and C) which manifests itself in the lowering of the chemical shifts.

Significantly more pronounced is the effect of the hydrogen bond length on the CSA values of the hydrogen and nitrogen nuclei. As the length changes from 2.57 Å to ∞, $|\text{CSA}_a|$ decreases by about 35 and 27 ppm for ^{15}N and ^{1}H, respectively. The dependence of both CSA_a(N) and CSA_a(H) values on the hydrogen bond length can be approximated by an exponential. However, the ^{1}H shielding depends strongly on stacking interactions (data not shown). Therefore, the values for ^{1}H in Table 1 should be interpreted qualitatively as general trends rather than as absolute values.

TABLE 1
Chemical Shielding Data of Guanine N1 and H1 in G–C Base Pair

$r_{N\ldots N}$ (Å)	δ (ppm)	σ_{11} (ppm)	σ_{22} (ppm)	σ_{33} (ppm)	θ_1 (°)	θ_2 (°)	θ_3 (°)	CSA_a (ppm)	$\Delta\eta$	$\Delta\sigma^*$ (ppm)
					N15					
2.57	140.2	37.2	90.6	186.7	28.1	118.0	87.9	−131.2	1.42	−83.5
2.72	137.9	40.1	101.3	180.1	22.5	112.3	87.7	−121.6	1.17	−87.0
2.87	136.3	42.0	110.4	173.9	18.9	108.7	87.6	−114.3	0.95	−89.2
3.02	135.1	43.4	118.1	168.4	16.6	106.4	87.5	−108.9	0.76	−90.6
3.17	134.6	44.2	124.1	163.2	14.9	104.7	87.4	−105.1	0.59	−91.4
3.5	133.5	46.2	133.7	154.8	12.9	102.6	87.1	−99.7	0.32	−91.4
∞	131.0	50.8	140.9	150.4	9.0	88.4	98.9	−95.2	0.15	−91.2
					H1					
2.57	20.1	−7.0	9.8	31.6	85.3	92.5	5.3	33.5	0.83	29.7
2.72	17.3	−1.3	13.0	30.8	85.8	92.3	4.9	27.8	0.86	24.6
2.87	15.3	3.1	15.5	30.2	86.1	92.2	4.5	23.5	0.89	20.7
3.02	13.7	6.4	17.2	29.8	86.3	92.1	4.3	20.3	0.91	17.8
3.17	12.6	8.9	18.6	29.4	86.6	92.1	4.0	17.8	0.92	15.6
3.5	7.2	18.0	24.2	31.0	87.3	92.3	3.6	11.2	0.94	9.8
∞	8.5	19.4	22.8	26.9	89.2	95.0	5.1	6.5	0.87	5.7

Note. $r_{N\ldots N}$ is the hydrogen bond length (GN1–CN3 distance) in the G–C base pair; σ_{11}, σ_{22}, and σ_{33} are the components of the shielding tensor; θ_1, θ_2, and θ_3 are the angles between the corresponding shielding component and the GN1–Himino vector. The isotropic chemical shifts of imino nitrogen $\delta(^{15}\text{N})$ and imino proton $\delta(^1\text{H})$ were obtained by subtracting the isotropic shieldings from the values of isotropic shieldings σ_{iso} (^{15}N) and σ_{iso} (^{1}H) for standards. σ_{iso} (^{15}N) = 245.07 ppm for ^{15}N in liquid NH_3 is an experimental value from the literature (*31*) and σ_{iso} (^{1}H) = 31.534 ppm for protons in TMS was calculated *ab initio* using the same approach as for the guanine imino proton. $\Delta\eta$, CSA_a, and $\Delta\sigma^*$ were calculated according to Eqs. [4], [5], and [7], respectively.

Not only the absolute value of CSA, but also the orientation of the ^{15}N chemical shift tensor depends on the length of the hydrogen bond. For a nitrogen nucleus not involved in hydrogen bonding, the shielding tensor is nearly axially symmetric with asymmetry factor $\Delta\eta = 0.15$, $\sigma_{\|} \equiv \sigma_{11}$ is almost collinear with the bond vector ($\theta_1 = 9.0°$), and the σ_{11} and σ_{22} component lie in the plane of the G base. As the length of the hydrogen bond decreases the least shielding component σ_{11} deflects from the N–H vector and the shielding tensor becomes increasingly asymmetric. For a hydrogen bond typical length of 2.87 Å, the angle θ_1 and the asymmetry factor reach the values of 18.9° and 0.95, respectively, with the most shielded component almost perpendicular to the base plane. At shorter hydrogen bond lengths, the larger value of θ_1 more than compensates for the greater absolute value of CSA_a. Consequently, the term $\Delta\sigma^*$, responsible for the cross-correlation, changes very little with the hydrogen bond length.

The orientation of the ^{1}H shielding tensor is rather different from that of ^{15}N. Here, the tensor is not even approximately axially symmetric for any length of the hydrogen bond and the shielding component closest to the N–H bond is σ_{33}. The angle, θ_3, between σ_{33} and the N–H bond is very small and neither the orientation of the shielding tensor nor its asymmetry factor depend significantly on the hydrogen bond length.

As pointed out recently (*4*), the noncollinearity of the ^{15}N chemical shift and ^{1}H–^{15}N dipolar tensors in combination with the anisotropy of the overall molecular motion has an effect on the TROSY linewidth, especially at very high magnetic fields. The three main parameters affecting the ^{15}N linewidth in a TROSY experiment are the CSA_a of the ^{15}N, the corresponding $\Delta\sigma^*$, and the distribution of distant protons around the ^{15}N–^{1}H spin pair. The absolute value of the CSA_a declines as the hydrogen bond length increases and therefore the contribution to the relaxation due to the CSA mechanism is smaller. The absolute value of the cross-correlation term, $\Delta\sigma^*$, increases somewhat for larger $r_{N\ldots N}$ making the TROSY mechanism more efficient. Finally, a longer hydrogen bond means a greater distance between the G imino proton and the amino protons of the cytosine in the base pair, which limits the effect of the proton–proton dipolar coupling. All three factors thus work in concert to produce narrower lines for longer hydrogen bonds. The effect is not dramatic, however, and will probably be noticeable only at very high (800 MHz) fields. The significantly lower value of $\Delta\sigma^*$ for G imino (~90 ppm) compared to that for the amide proton in proteins (~140 ppm) suggests that the efficiency of TROSY for ^{15}N in G is lower and requires higher fields. As noted before (*4*), the noncollinearity of the dipolar and shielding tensors means that the minimal linewidth is achieved at a lower field but the line narrowing is not that pronounced. Our calculations show that for $r_{N\ldots N} \rightarrow \infty$ the optimum requires as high a field as 1.7 GHz. Only for very short hydrogen bond lengths (2.57 Å) does the optimal frequency approach 800 MHz.

Besides the stem regions with hydrogen bonded base pairs, molecules of nucleic acids often contain loops and bulges where the imino protons are involved in weak or no hydrogen bonding. Table 1 shows a difference of about 20 ppm in CSA_a between a nitrogen atom involved in a typical hydrogen bond and a nonbonded nitrogen atom. For shorter hydrogen bonds, the difference can be as large as 35 ppm. According to numerical simulations (*29*), the effect of the variation of ^{15}N CSA on the calculated order parameters ΔS^2 can be described by the equation $\Delta S^2 = [0.0015\ (\Delta\sigma + 100)]\ S^2$ over the ranges $S^2 \in \langle 0.6, 0.9\rangle$ and $|\Delta\sigma| \in \langle 80\text{ ppm}, 120\text{ ppm}\rangle$ at 500 MHz. Using the uniform values of $\Delta\sigma$ for all imino nitrogens irrespective of the effect of the hydrogen bonding may introduce systematic errors of 3 to 5% in determining S^2 from the data measured at 500 MHz. Since the relaxation effects due to CSA depend on the square of the magnetic field, the effect becomes more pronounced with higher fields. With base-to-base variations of S^2 typically about 10%, the introduced errors may reach the same magnitude as the differences in S^2 due to molecular motions if the relaxation parameters are measured at fields of 600 MHz or higher. Therefore, it is essential to take into account the differences in ^{15}N CSA due to hydrogen bonding effects when interpreting high-field relaxation data in terms of molecular dynamics. On the other hand, the variation in the term responsible for ^{15}N cross-correlation, $\Delta\sigma^*$, only amounts to approximately 5% of the difference between the extreme values in Table 1. We can therefore expect that if uniform values of CSA and/or $\Delta\sigma^*$ are used for all residues in the molecule, the parameters of molecular motion based on cross-correlation rates (*30*) would provide more accurate values than those based on auto-relaxation rates.

In conclusion, we have presented the results of systematic *ab initio* calculations of ^{1}H and ^{15}N shielding tensors in a GC base pair as a function of the hydrogen bond lengths. The ^{15}N shielding tensor of N_1, which in free guanine is almost axially symmetric ($\Delta\eta = 0.15$) and nearly collinear ($\theta_1 = 9°$) with the N–H bond vector, becomes asymmetric when the base is involved in the hydrogen bonding. The parameters characterizing the shielding anisotropy $\Delta\eta$ and θ_1 exponentially increase as the length of the hydrogen bond decreases. As discussed, the shielding asymmetry must be considered in the analysis of relaxation behavior, the extraction of motional parameters, and the evaluation of TROSY effects.

ACKNOWLEDGMENTS

This research has been supported by the Grant Agency of the Czech Republic, Grant 203/99/0311, and by the Ministry of Education of the Czech Republic, Grants VS96095 and J07/98:143100005.

REFERENCES

1. M. W. F. Fischer, A. Majumdar, and E. P. R. Zuiderweg, Protein NMR relaxation: Theory, applications and outlook, *Prog. NMR Spectrosc.* **33,** 207–272 (1998).
2. D. Fushman and D. Cowburn, Model Independent Analysis of ^{15}N Chemical Shift Anisotropy from NMR Relaxation Data. Ubiquitin as

a Test Sample, *J. Am. Chem. Soc.* **120,** 7109–7110 (1998); J. Boyd and C. Redfield, Defining the Orientation of the ^{15}N Shielding Tensor Using ^{15}N Relaxation Data for a Protein in Solution, *J. Am. Chem. Soc.* **120,** 9692–9693 (1998).

3. D. Fushman, N. Tjandra, and D. Cowburn, Direct Measurement of ^{15}N Chemical Shift Anisotropy in Solution, *J. Am. Chem. Soc.* **120,** 10947–10952 (1998).
4. D. Fushman and D. Cowburn, The effect of noncollinearity of ^{15}N dipolar and ^{15}N CSA tensors and rotational anisotropy on ^{15}N relaxation, CSA/dipolar cross-correlation, and TROSY, *J. Biomol. NMR* **13,** 139 (1999).
5. K. Pervushin, R. Riek, G. Wider, and K. Wüthrich, Attenuated T_2 relaxation by mutual cancellation of dipole–dipole and chemical shift anisotropy indicates an avenue to NMR structures of very large biological macromolecules in solution, *Proc. Natl. Acad. Sci. USA* **94,** 12366–12371 (1997); R. Riek, G. Wider, K. Pervushin, and K. Wüthrich, Polarization transfer by cross-correlated relaxation in solution NMR with very large molecules, *Proc. Natl. Acad. Sci. USA* **96,** 4918–4923 (1999).
6. K. Wüthrich, "NMR of Proteins and Nucleic Acids," Wiley, New York (1986).
7. J. Jursa and J. Kypr, Geometries and energies of Watson–Crick base pairs in oligonucleotide crystal structures, *Gen. Physiol. Biophys.* **12,** 401–419 (1993).
8. K. Pervushin, A. Ono, C. Fernández, T. Szyperski, M. Kainosho, and K. Wüthrich, NMR scalar coupling across Watson-Crick base pair hydrogen bonds in DNA observed by transverse relaxation-optimized spectroscopy, *Proc. Natl. Acad. Sci. USA* **95,** 14147–14151 (1998).
9. A. J. Dingley, J. E. Masse, R. D. Peterson, M. Barfield, J. Feigon, and S. Grzesiek, Internuclear scalar couplings across hydrogen bonds in Watson–Crick and Hoogsteen base pairs of a DNA triplex, *J. Am. Chem. Soc.* **121,** 6019–6027 (1999).
10. D Sitkoff and D. Case, Theories of chemical shift anisotropies in proteins and nucleic acids, *Proc. Nucl. Magn. Spectrosc.* **32,** 165–190 (1998).
11. K. L. Anderson-Altmann, C. G. Phung, S. Mavromoustakos, Z. Zheng, J. C. Facelli, C. D. Poulter, and D. M. Grant, ^{15}N chemical shift tensors of uracil determined from ^{15}N powder pattern and ^{15}N–^{13}C dipolar NMR spectroscopy, *J. Phys. Chem.* **99,** 10454–10458 (1995).
12. J. Z. Hu, J. C. Facelli, D. W. Alderman, R. J. Pugmire, and D. M. Grant, ^{15}N chemical shift tensors in nucleic acid bases, *J. Am. Chem. Soc.* **120,** 9863–9869 (1998).
13. The structure ID:BDL001 is a B-DNA double helix. Residues 4 (G) and 21 (C) were selected.
14. D. R. Salahub, R. Fournier, P. Mlynarski, A. Papai, A. St-Amant, and J. Uskio, Gaussian-based density functional methodology, software, and applications, *in* "Density Functional Methods in Chemistry" (J. Labanowski and J. W. Andzelm, Eds.), pp. 77–100, Springer-Verlag, New York (1991).
15. V. G. Malkin, O. L. Malkina, and D. R. Salahub, "MASTER-CS Program," Universite de Montreal, Montreal (1994).
16. J. P. Perdew and Y. Wang, Accurate and simple analytic representation of the electron-gas correlation energy, *Phys. Rev. B* **45,** 13244–13249 (1992).
17. J. P. Perdew, J. A. Chevary, S. H. Vosko, K. A. Jackson, M. R. Pederson, D. J. Singh, and C. Fiolhais, Atoms, molecules, solids, and surfaces: Applications of the generalized gradient approximation for exchange and correlation, *Phys. Rev. B* **46,** 6671–6687 (1992).
18. V. G. Malkin, O. L. Malkina, L. A. Eriksson, and D. R. Salahub, The calculation of NMR and EPR parameters using density functional theory, *in* "Theoretical and Computational Chemistry" (J. M. Seminario and P. Politzer, Eds.), pp. 273–347, Elsevier, Amsterdam (1995).
19. V. G. Malkin, O. L. Malkina, M. E. Casida, and D. R. Salahub, Nuclear magnetic resonance shielding tensors calculated with sum-over-states density functional perturbation theory, *J. Am. Chem. Soc.* **116,** 5898–5908 (1994).
20. W. Kutzelnigg, U. Fleischer, and M. Schindler, The IGLO-method: Ab-initio calculation and interpretation of NMR chemical shifts and magnetic susceptibilities, *NMR Basic Principles Progress* **23,** 167–262 (1990).
21. M. J. Frish, G. W. Truck, H. B. Schlegel, P. M. W. Gill, B. G. Johnson, M. A. Robb, J. R. Cheeseman, T. Keith, G. A. Petersson, J. A. Montgomery, K. Raghavachari, M. A. Al-Laham, V. G. Zakrzewski, J. V. Ortiz, J. B. Foresman, J. Cioslowski, B. B. Stefanov, A. Nanayakkara, M. Challacombe, C. Y. Peng, P. Y. Ayala, W. Chen, M. W. Wong, J. L. Andres, E. S. Replongle, R. Gomperts, R. L. Martin, D. J. Fox, J. S. Binkley, D. J. Defrees, J. Baker, J. P. Stewart, M. Head-Gordon, C. Gonzales, and J. A. Pople, "Gaussian 94, Revision C.2," Gaussian, Inc., Pittsburgh (1995).
22. J. R. Cheeseman, G. W. Trucks, T. A. Keith, and M. J. Frish, A comparison of models for calculating nuclear magnetic resonance shielding tensors, *J. Chem. Phys.* **104,** 5497–5509 (1996).
23. A. D. Becke, Density-functional thermochemistry. III. The role of exact exchange, *J. Chem. Phys.* **98,** 5648–5652 (1992).
24. A. Schäfer, H. Horn, and R. Ahlrichs, Fully optimized contracted Gaussian basis sets for atoms Li to Kr, *J. Chem. Phys.* **97,** 2571–2577 (1992).
25. J. Czernek and V. Sklenář, Ab initio calculations of ^{1}H and ^{13}C chemical shifts in anhydrodeoxythymidines, *J. Phys. Chem. A* **103,** 4089–4093 (1999).
26. P. Damberg, J. Jarvet, P. Allard, and A. Gräslund, Quantitative estimation of magnitude and orientation of CSA tensor from field dependence of longitudinal NMR relaxation rates, *J. Biomol. NMR* **15,** 27–37 (1999).
27. W. Saenger, "Principles of Nucleic Acid Structure," Springer-Verlag, New York (1983).
28. F. Jiang, R. Fiala, D. Live, R. A. Kumar, and D. J. Patel, RNA folding topology and intermolecular contacts in the AMP-RNA aptamer complex, *Biochemistry* **35,** 13250–13266 (1996).
29. M. Akke, R. Fiala, F. Jiang, D. Patel, and A. G. Palmer, Base dynamics in a UUCG tetraloop RNA hairpin characterized by ^{15}N spin relaxation: Correlations with structure and stability, *RNA* **3,** 702–709, (1997).
30. C. D. Kroenke, J. P. Loria, L. K. Lee, M. Rance, and A. G. Palmer, III, Longitudinal and transverse ^{1}H–^{15}N dipolar/^{15}N chemical shift anisotropy relaxation interference: Unambiguous determination of rotational diffusion tensors and chemical exchange effects in biological macromolecules, *J. Am. Chem. Soc.* **120,** 7905–7915 (1998).
31. C. J. Jameson and A. C. de Dios, Nuclear magnetic shielding of nitrogen in ammonia, *J. Chem. Phys.* **95,** 1069–1079 (1991).